1,3-Adamantane-3,13-Porphyrin-6,6-Cyclophane: Crystal Structure of the Free Base and Steric Effects on Ligation of the Iron(II) Complex

T. G. Traylor,*† N. Koga,† L. A. Deardurff,† Paul N. Swepston,‡ and James A. Ibers*‡

Contribution from the Departments of Chemistry, University of California, San Diego, La Jolla, California 92093, and Northwestern University, Evanston, Illinois 60201.
Received September 20, 1983

Abstract: The coupling of 1,3-adamantanediacetyl chloride to 8,18-bis(2-carbobenzoxyethyl)-3,13-bis(o-aminopropyl)-2,7,12,17-tetramethylporphyrin affords 1,3-adamantane-3,13-porphyrin-6,6-cyclophane. The material crystallizes as the bis(dichloromethane) solvate, $C_{64}H_{72}N_6O_6 \cdot 2CH_2Cl_2$, in space group C_i^1-$P\bar{1}$ of the triclinic system with two formula units in a cell of dimensions a = 15.858 (28) Å, b = 17.779 (32) Å, c = 12.970 (24) Å, α = 109.62 (6)°, β = 97.88 (7)°, γ = 114.18 (7)°, and V = 2977 Å^3. The structure was described by 742 variables, and at convergence of the full-matrix least-squares refinement the values of R and R_w (on F^2, 7749 unique data) are 0.093 and 0.168. The conventional R index on F for 5489 reflections having $F_o^2 > 3\sigma(F^2)$ is 0.065. The porphyrin macrocycle is approximately planar, with the mean displacement from the 24-atom plane being 0.038 Å and the maximum displacement being 0.101 (4) Å. As a whole, the molecule is relatively unstrained. In the solid state the adamantane bridge has an offset orientation relative to the plane of the porphyrin and short intramolecular contacts that indicate no free cavity between the strap and the porphyrin. NMR spectroscopic results show that in solution the adamantane flips rapidly between two asymmetric orientations. The (dicyclohexylimidazole)iron(II) complex of the porphyrin binds CO, O_2, and isocyanides with greatly reduced affinities compared with open heme compounds. A small steric differentiation between CO and O_2 is demonstrated, and variations in the magnitude of steric effects are found to depend upon the nature of the hindering group.

The control of dioxygen and other ligand binding to heme proteins is a subject of great current interest.[1-4] One factor that has received considerable attention in theoretical as well as experimental studies on both heme proteins and model compounds is the steric interference to ligation that accrues from having some bulky group near the position that is assumed by the bound ligand.[5-10] This phenomenon is referred to as the distal-side steric effect to differentiate it from other steric effects that introduce strain, doming, or other distortions into the porphyrin structure.

Heme proteins are known to bind isocyanides with greatly reduced affinities[11] compared with simple model compounds[12] and to display decreasing affinities with increasing isocyanide size. Variations in relative affinities of carbon monoxide and dioxygen or nitric oxide in different heme proteins,[1,13] along with the "bent" geometry of bound carbon monoxide in these positions,[3] have been interpreted in terms of steric differentiation of carbon monoxide and dioxygen by some[13,14] or all heme proteins.[6,15]

Steric hindrance to carbon monoxide, dioxygen, isocyanides, and amines has been demonstrated with a variety of heme-cyclophanes[5-8] and it has been established that such steric effects do not appreciably affect dissociation rates of ligands, even for highly reduced binding.[5,7] However, conclusions with regard to the steric differentiation of CO and O_2 vary. We have reported an approximately 300-fold reduction compared with the open heme complexes in CO and O_2 binding to anthracene-6,6-cyclophane (**1a**, Chart I)[16] with no differentiation between them.[7] Ward et al.[5] report a somewhat greater steric effect on carbon monoxide than on dioxygen binding to 15-heme-cyclophane (**2a**). Collman et al.[6] report a 70-fold reduction in CO binding and no change in O_2 binding upon comparing tetrakis[α-(*o*-pivalamidophenyl)]heme to the capped "pocket heme" **3**, concluding that steric effects were responsible for differentiation. Rose et al.,[9a] upon comparing the kinetics and equilibria for carbon monoxide binding to the capped hemes **4a,b** with those for the parent tetraphenylheme, concluded that these capped hemes show no steric hindrance to CO binding.

One of the problems with these interpretations is the sensitivity of both CO and O_2 binding to other steric (strain) effects[17,18] and the sensitivity of dioxygen binding to electronic and solvent effects.[17b,18] Thus, a new cyclophane structure might alter local solvation or electronic effects sufficiently to change O_2 affinity in the direction opposite to that of the designed steric effects.

†University of California, San Diego.
‡Northwestern University.

(1) Moffat, K.; Deatherage, J. F.; Seybert, D. W. *Science (Washington, D.C.)* **1979**, *206*, 1035-1042.
(2) Chevion, M.; Salhany, J. M.; Peisach, J.; Castillo, C. L.; Blumberg, W. E. *Isr. J. Chem.* **1977**, *15*, 311-317.
(3) Baldwin, J. M. *J. Mol. Biol.* **1980**, *136*, 103-128.
(4) Perutz, M. F. *Annu. Rev. Biochem.* **1979**, *48*, 327-386.
(5) Ward, B.; Wang, C.; Chang, C. K. *J. Am. Chem. Soc.* **1981**, *103*, 5236-5238.
(6) (a) Collman, J. P.; Brauman, J. I.; Collins, T. J.; Iverson, B.; Sessler, J. L. *J. Am. Chem. Soc.* **1981**, *103*, 2450-2452. (b) Collman, J. P.; Brauman, J. I.; Iverson, B. L.; Sessler, J. L.; Morris, R. M.; Gibson, Q. H. *Ibid.* **1983**, *105*, 3052-3064.
(7) Traylor, T. G.; Mitchell, M. J.; Tsuchiya, S.; Campbell, D. H.; Stynes, D. V.; Koga, N. *J. Am. Chem. Soc.* **1981**, *103*, 5234-5236.
(8) Busch, D. H.; Zimmer, L. L.; Grzybowski, J. J.; Olszanski, D. J.; Jackels, S. C.; Callahan, R. C.; Christoph, G. G. *Proc. Natl. Acad. Sci. U.S.A.* **1981**, *78*, 5919-5923.
(9) (a) Rose, E. J.; Venkatasubramanian, P. N.; Swartz, J. C.; Jones, R. D.; Basolo, F.; Hoffman, B. M. *Proc. Natl. Acad. Sci. U.S.A.* **1982**, *79*, 5742-5745. (b) Hashimoto, T.; Basolo, F. *Comments Inorg. Chem.* **1981**, *1*, 199-205.
(10) Case, D. A.; Karplus, M. *J. Mol. Biol.* **1979**, *132*, 343-368.
(11) Reisberg, P. I.; Olson, J. S. *J. Biol. Chem.* **1980**, *255*, 4159-4169.
(12) Traylor, T. G.; Stynes, D. V. *J. Am. Chem. Soc.* **1980**, *102*, 5938-5939.
(13) Caughey, W. S. *Ann. N.Y. Acad. Sci.* **1970**, *174*, 148-153.
(14) White, D. K.; Cannon, J. B.; Traylor, T. G. *J. Am. Chem. Soc.* **1979**, *101*, 2443-2454.
(15) Romberg, R. W.; Kassner, R. J. *Biochemistry* **1979**, *18*, 5387-5392. These authors more recently observed the K^{NO}/K^{CO} for human hemoglobin to be similar to that for their hemin-1-methylimidazole model compound. (R.J.K., private communication.)
(16) Abbreviations and definitions: Hb = hemoglobin; TMIC = *p*-toluenesulfonylmethyl isocyanide; *n*-BuNC = *n*-butyl isocyanide; MeIm = 1-methylimidazole; 1,2-DMIm = 1,2-dimethylimidazole; DCIm = 1,5-dicyclohexylimidazole; **5** represents the four-coordinate Fe^{II} adamantane-porphyrin having the structure shown in eq 1, **5**$^+$Cl$^-$ is the corresponding hemin chloride, **5**P is the porphyrin, and **5**-MeIm is the five-coordinate Fe^{II} complex with 1-methylimidazole. In an *n*-cyclophane, *n* refers to the number of atoms in a single chain from one porphyrin edge to another. In *n,n,n*...cyclophanes, *n* refers to the number of atoms in each of the two or more chains connecting the porphyrin ring to the second aromatic ring. The kinetic and equilibrium constants for adding a ligand to a four- or five-coordinate heme are defined as K_B^A or K_B^{-A}, where the subscript (B) refers to the ligand that does not change and the superscript to that which is added or is lost (-A). In replacement reactions, A replaces C in $K_B^{C,A}$.
(17) (a) Collman, J. P. *Acc. Chem. Res.* **1977**, *10*, 265-272. (b) Traylor, T. G. *Ibid.* **1981**, *14*, 102-109.

0002-7863/84/1506-5132$01.50/0

Chart I

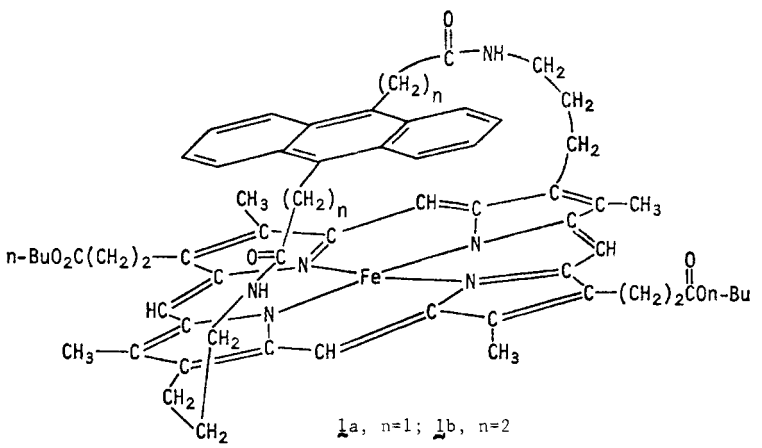

1a, n=1; 1b, n=2

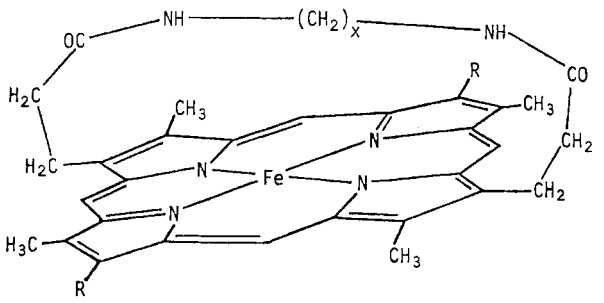

R = n-pentyl

2a, x = 5

2b, x = 7

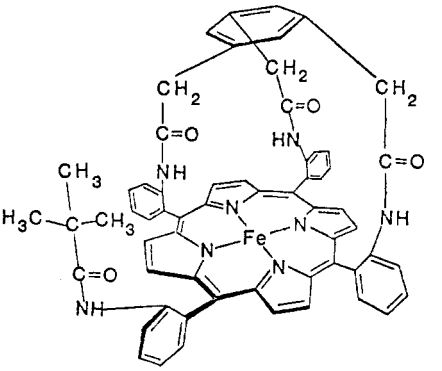

3

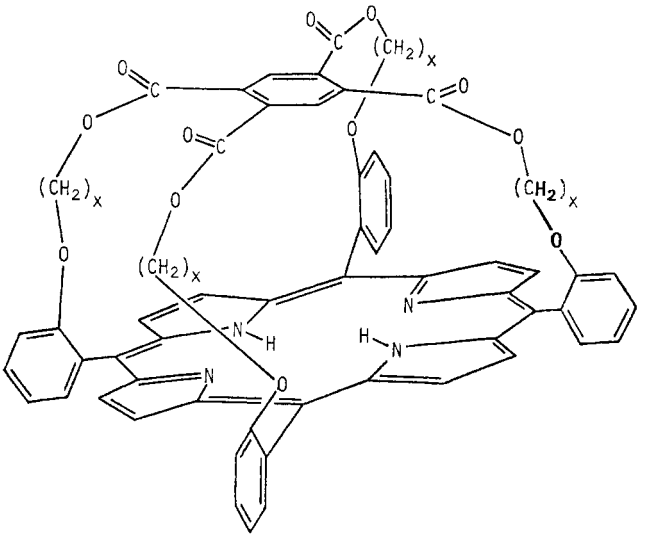

4a, x = 2

4b, x = 3

In an attempt to clarify this situation we have prepared an adamantane–cyclophane (**5**) that furnishes a bulky, nonaromatic group in the position very similar to that of the distal imidazole group in myoglobin. We have used kinetic criteria to demonstrate that this compound does not differ significantly with regard to local solvation or electronic effects from simple heme compounds. The crystal structure of the porphyrin free base and detailed kinetics studies of CO and O_2 binding to the (dicyclohexylimidazole)iron(II) complex afford definitive estimates of CO and O_2 steric effects.

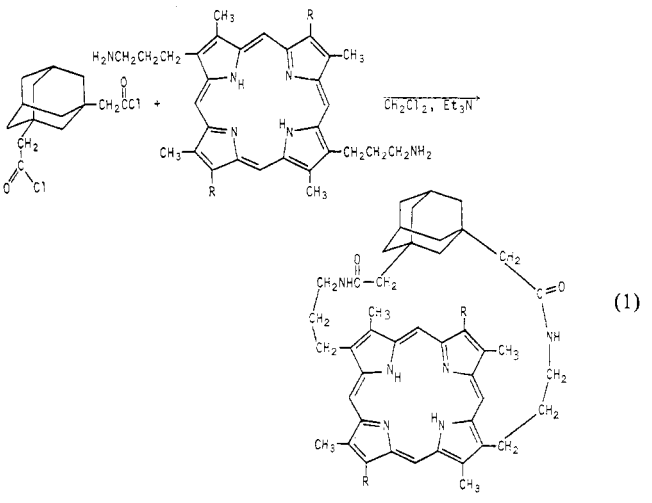

(1)

5a

R = $CH_2CH_2\overset{O}{\overset{\|}{C}}-OCH_2Ph$

Experimental Section

Reagents. Toluene (Mallinckrodt) was purified by the literature method,[19] except that it was distilled from calcium hydride (Aldrich) and stored over 4-Å molecular sieves. Except for methylene chloride (Mallinckrodt) and triethylamine (Aldrich), which were distilled from calcium hydride, and 1-methylimidazole (Aldrich), which was distilled at reduced pressure, all other solvents and reagents were used as received. All column chromatography used 60–200-mesh silica gel grade H from Davison Chemical Co.

Spectroscopic and Kinetic Instrumentation. The reported UV–visible spectra were determined on either a Cary 15 or Kontron Uvicon 810 spectrometer. The 360-MHz NMR and fast-kinetic instrumentation is described elsewhere.[20]

Kinetic Methods. Kinetics of the reaction of carbon monoxide and dioxygen with the 1,5-dicyclohexylimidazole (DCIm) complex of adamantane–heme–cyclophane (**5**) were determined in toluene by the method reported for the anthracene–cyclophanes.[7] Solutions of the imidazole–adamantane–heme–CO complexes were made by adding saturated sodium dithionite (Fisher) in 0.05 M sodium borate buffer (Mallinck-

(18) Jameson, G. B.; Ibers, J. A. *Comments Inorg. Chem.* **1983**, *2*, 97–126.

(19) Riddick, J. A.; Bunger, W. B. "Organic Solvents. Physical Properties and Methods of Purification", 3rd ed.; Wiley: New York, 1970; p 611.

(20) (a) Traylor, T. G.; Chang, C. K.; Geibel, J.; Berzinis, A.; Mincey, T.; Cannon, J. *J. Am. Chem. Soc.* **1979**, *101*, 6716–6731. (b) Traylor, T. G.; Mitchell, M.; Koga, N.; Stynes, D. *Ibid.*, submitted.

Table I. Crystallographic Details for 1,3-Adamantane-3,13-Porphyrin-6,6-Cyclophane

formula	$C_{64}H_{72}N_6O_6 \cdot 2CH_2Cl_2$
formula wt, amu	1191.19
space group	C_i^1-$P\bar{1}$
a, Å	15.858 (28)
b, Å	17.779 (32)
c, Å	12.970 (24)
α, deg	109.62 (6)
β, deg	97.88 (7)
γ, deg	114.18 (7)
vol, Å^3	2977
Z	2
density (calcd, −152 °C), g/cm^3	1.33
radiation	Mo Kα (λ(Kα_1) = 0.7093 Å), graphite monochromator
linear absorp coeff, cm^{-1}	2.54
temp,[a] °C	−152
detector aperture	5.4 mm wide × 6.0 mm high; 32 cm from crystal
take-off angle, deg	3.1
scan speed, deg/min	2 in 2θ
2θ limits, deg	$3.5 \leq 2\theta \leq 45.0$
scan range, deg	1.10 below Kα_1 to 1.30 above Kα_2
bkgd counts, s	10 at each end of scan with rescan option[b]
data collected	$\pm h, \pm k, +l$
unique data (including $F_o^2 < 0$)	7749
unique data with $F_o^2 > 3\sigma(F_o^2)$	5489
final no. of variables	742
$R(F^2)$	0.093
$R_w(F^2)$	0.168
error in an observation of unit weight, e^2	1.87
R(on F for $F_o^2 > 3\sigma(F_o^2)$)	0.065

[a] The low-temperature system is based on a design by: Huffman, J. C. Ph.D. Thesis, Indiana University, 1974. [b] The diffractometer was run under the Vanderbilt disk-oriented system (Lenhert, P. G. *J. Appl. Crystallogr.* **1975**, *8*, 568–570).

rodt) either to a concentrated solution of the hemin **5** in 0.2 mL of toluene/DCIm or to an approximately 10 μM hemin solution that was 0.45 M in DCIm. During this and the subsequent preparation steps, all solutions were deoxygenated by passing CO gas through them for 10–30 min. For reduction as a concentrated solution, 20–60 μL of the solution was transferred to 3 mL of 0.45 M DCIm solution in a 130-mL tonometer. For reduction of the dilute solution the organic phase was transferred to the tonometer. An equal volume of deoxygenated toluene was added to the tonometer and then removed by passing CO gas through it to dry the solution. The solution was then degassed by freeze–thaw cycles, and the tonometer was filled with argon or left under vacuum. Carbon monoxide and dioxygen were added to the tonometer with gastight syringes and equilibrated with stirring at the reaction temperature for 20 min. The solubilities of carbon monoxide and dioxygen were taken as 1×10^{-5} and 1.2×10^{-5} M torr^{-1}, respectively.[18,21] Flash photolysis kinetic measurements were performed as previously described[20] with the use of either a Phase-R 2100D laser or a Sunpak 611 flash gun and microprocessor-controlled transient recorder.

X-ray Study of the Free Base. Crystals of $C_{64}H_{72}N_6O_6 \cdot 2CH_2Cl_2$ suitable for X-ray work were obtained through recrystallization from CH_2Cl_2. The crystals belong to the triclinic system as deduced from preliminary photographic examination. Accurate unit cell parameters were determined by least-squares refinement of 16 reflections ($26.0 < 2\theta < 30.0°$) that had been automatically centered on a Picker FACS-I diffractometer. Data collection was performed at −152 °C in a manner standard in this laboratory.[22] Six standard reflections measured at 100-reflection intervals showed no indication of crystal decay during the course of data collection. Crystallographic and experimental details are given in Table I.

In spite of analytical and spectral evidence for two solvent molecules per asymmetric unit, it was not possible to identify Cl–Cl vectors in a sharpened Patterson map. MULTAN80[23] was subsequently employed in the solution of this structure. Normalized structure factors were calculated with molecular scattering factors being used for a porphyrin, a phenyl, and an adamantane fragment. Since intensity statistics favored space group $P\bar{1}$, it was chosen as the correct group. No recognizable molecular fragment was found in a search of the four phase sets with the highest combined figures of merit. However, there was a paucity of σ-2 relationships despite the fact that the maximum number of E values was already being used in the standard program. MULTAN80 was therefore redimensioned so that a greater number of E values could be employed in the phasing process; a 36% increase in the number of E values led to a 138% increase in the number of triplet relationships. A 17-atom starting model containing two complete pyrrole rings was located in an E map calculated from the fourth best phase set of a subsequent calculation. After two iterations of Karle recycling,[24] the model had been extended to 29 atoms. A combination of Sim-weighted Fourier calculations and Karle recycling was then employed to develop the model to 63 atoms, but the phenyl carbon atoms and one carbon atom of the adamantane "cap" could not be located. Least-squares refinement of this model led to large residuals (R = 63%) and the conclusion that the fragment was properly oriented but misplaced with respect to the inversion center. Its correct position was eventually determined by treating the known fragment as if it were in space group $P1$.[25] An electron density calculation based on the 31-atom fragment revealed a fragment of the second molecule and consequently the location of the inversion center. All of the 76 non-hydrogen atoms of the porphyrin and two solvent molecules were now readily located after a weighted electron density calculation based on space group $P\bar{1}$. In a reexamination of the sharpened Patterson map, one of the intramolecular Cl–Cl vectors was identified as the 86th largest peak while the other intramolecular Cl–Cl vector was not found among the 100 largest peaks.

Standard procedures and programs were used to develop and refine the model.[22] Isotropic refinement of the porphyrin atoms and anisotropic refinement of the solvent atoms led to values of R and R_w on F_o of 0.13 and 0.16. Hydrogen atoms were added as fixed contributions to the structure factors and updated before each subsequent cycle of refinement. Pyrrole hydrogen positions were obtained from a difference electron density synthesis, idealized methyl hydrogen positions (C–H = 0.95 Å; H–C–H = 109.5°) were obtained from a least-squares adjustment of their observed positions, and the remaining hydrogen positions were calculated by assuming idealized geometries. Each hydrogen atom was assigned an isotropic thermal parameter 1 Å^2 greater than the equivalent isotropic thermal parameter of the atom to which it is attached.

In the final cycles of refinement, all non-hydrogen atoms were refined anisotropically and the occupancies of the solvate molecules were varied. The final cycle of refinement on F_o^2 involved 742 variables and 7753 unique intensities (including those for which $F_o^2 < 0$). The final residuals are $R(F_o^2)$ = 0.093 and $R_w(F_o^2)$ = 0.168 and the error in an observation of unit weight is 1.87 e^2. The conventional R indices on F_o for the 5488 reflections having $F_o^2 > 3\sigma(F_o^2)$ are $R(F_o)$ = 0.065 and $R_w(F_o)$ = 0.081. The six largest peaks in the final difference map (0.5 (1)–1.0 (1) e/Å^3) are located near the chlorine atoms of the solvate molecules but are not interpretable in terms of solvate disorder. The refined occupancies of the solvate molecules are 0.97 (1) and 0.93 (1), and hence we take the complex to be the bis(solvate).

The positional parameters for the non-hydrogen atoms are listed in Table II. Table III presents the anisotropic thermal parameters,[26] Table IV presents the hydrogen atom parameters,[26] and Table V presents the final values of $100|F_o|$ and $100|F_c|$.[26]

Syntheses. Adamantane–Porphyrin–6,6-Cyclophane ([8,18-Bis(2-carbobenzoxyethyl)-2,7,12,17-tetramethylporphyrin-3,13]-Adamantane-1,3-[6(2-Oxo-3-aza),6(2-oxo-3-aza)-cyclophane]) (5P). 1,3-Adamantanediacetyl chloride (**2**) was prepared by treating 60 mg of 1,3-adamantanediacetic acid (Aldrich) with 4 mL of thionyl chloride (Mallinckrodt). After refluxing for 30 min, removing the thionyl chloride under vacuum, dissolving the product in methylene chloride, and reevacuating under high vacuum, we used the product without further pu-

(21) (a) Lemke, W. F. "Solubilities of Inorganic and Metal Organic Compounds"; Van Nostrand: New York, 1958. (b) Schäfer, K.; Lax, E. "Landolt Bornstein Tables"; Springer-Verlag: Berlin, 1962; Vol. 2, Part 2, pp 1–89.

(22) See, for example: Waters, J. M.; Ibers, J. A. *Inorg. Chem.* **1977**, *16*, 3273–3277.

(23) Main, P.; Fiske, S. J.; Hull, S. E.; Lessinger, L.; Germain, G.; Declerq, J.-P.; Woolfson, M. M. "MULTAN80. A System of Computer Programs for the Automatic Solution of Crystal Structures from X-ray Diffraction Data"; Universities of York, England, and Louvain, Belgium.

(24) Karle, J. In "Crystallographic Computing Techniques"; Ahmed, F. R., Huml, K., Sedlacek, B., Eds.; Munksgaard: Copenhagen, 1976, pp 155–164.

(25) For examples of this procedure see: Flippen, J. L.; Gilardi, R. D. *Acta Crystallogr., Sect. B* **1975**, *B31*, 926–928; Karle, I. L.; Karle, J. *Ibid.* **1971**, *B27*, 1891–1898.

(26) Supplementary material.

Table II. Positional Parameters[a] for the Non-Hydrogen Atoms of 1,3-Adamantane-3,13-Porphyrin-6,6-Cyclophane

atom	x	y	z	atom	x	y	z
Cl(1)	0.91383 (11)	0.77150 (13)	0.48985 (14)	C(26)	1.29556 (36)	1.26527 (31)	1.19327 (41)
Cl(2)	0.96655 (12)	0.72002 (12)	0.28339 (17)	C(27)	1.34877 (35)	1.28920 (32)	1.12268 (46)
Cl(3)	0.25857 (15)	0.49862 (14)	0.93015 (16)	C(28)	1.30433 (40)	1.29284 (35)	1.02646 (44)
Cl(4)	0.44537 (14)	0.65624 (14)	1.00297 (22)	C(29)	1.20628 (37)	1.26967 (35)	0.99892 (39)
O(1)	1.02193 (21)	1.04669 (21)	1.14327 (27)	C(30)	1.15399 (33)	1.24543 (32)	1.07049 (40)
O(2)	1.04429 (21)	1.18933 (20)	1.20882 (26)	C(31)	0.23237 (29)	0.82776 (29)	0.27046 (34)
O(3)	0.07710 (26)	0.76055 (25)	0.06613 (31)	C(32)	0.18665 (30)	0.73231 (30)	0.17464 (35)
O(4)	0.03995 (21)	0.61731 (22)	0.03151 (26)	C(33)	0.09659 (29)	0.70814 (33)	0.08696 (36)
O(5)	0.23448 (26)	0.48842 (23)	0.61197 (31)	C(34)	−0.05242 (33)	0.58269 (36)	−0.05494 (41)
O(6)	0.63461 (27)	0.64100 (23)	0.21466 (30)	C(35)	−0.04624 (30)	0.55712 (33)	−0.17376 (38)
N(1)	0.60298 (23)	0.91785 (21)	0.80713 (26)	C(36)	−0.03722 (34)	0.48126 (35)	−0.22635 (45)
N(2)	0.40535 (23)	0.87057 (21)	0.69781 (28)	C(37)	−0.04702 (42)	0.44648 (42)	−0.33914 (56)
N(3)	0.45032 (24)	0.88567 (21)	0.49149 (27)	C(38)	−0.06508 (43)	0.48665 (60)	−0.40391 (50)
N(4)	0.64908 (23)	0.93436 (21)	0.60230 (28)	C(39)	−0.06864 (36)	0.56717 (56)	−0.35288 (64)
N(5)	0.28523 (26)	0.63763 (25)	0.70602 (32)	C(40)	−0.05842 (33)	0.60195 (35)	−0.23698 (48)
N(6)	0.70854 (26)	0.78399 (25)	0.35326 (30)	C(41)	0.24851 (30)	0.79514 (30)	0.87607 (36)
C(1)	0.70003 (27)	0.94221 (26)	0.83981 (32)	C(42)	0.24279 (32)	0.70660 (33)	0.87450 (39)
C(2)	0.72402 (29)	0.94665 (27)	0.95292 (33)	C(43)	0.20671 (31)	0.62945 (31)	0.75534 (39)
C(3)	0.64252 (29)	0.92727 (27)	0.98673 (34)	C(44)	0.29718 (32)	0.56802 (32)	0.64505 (39)
C(4)	0.56562 (29)	0.90860 (27)	0.89369 (34)	C(45)	0.39266 (31)	0.59407 (30)	0.62221 (38)
C(5)	0.46901 (29)	0.88159 (27)	0.88739 (34)	C(46)	0.80283 (30)	0.99444 (30)	0.41460 (38)
C(6)	0.39285 (28)	0.86057 (27)	0.79536 (34)	C(47)	0.82570 (31)	0.92280 (33)	0.34414 (38)
C(7)	0.29060 (28)	0.82363 (27)	0.79101 (35)	C(48)	0.74109 (37)	0.82749 (34)	0.27796 (39)
C(8)	0.24238 (27)	0.81281 (27)	0.68773 (34)	C(49)	0.65460 (32)	0.69297 (34)	0.31393 (45)
C(9)	0.31417 (28)	0.84153 (26)	0.63091 (32)	C(50)	0.62459 (33)	0.66230 (30)	0.40489 (40)
C(10)	0.29216 (28)	0.83803 (26)	0.52016 (33)	C(51)	0.50258 (29)	0.62628 (27)	0.50634 (36)
C(11)	0.35299 (26)	0.85813 (26)	0.45671 (31)	C(52)	0.51466 (30)	0.62787 (28)	0.39200 (36)
C(12)	0.33101 (29)	0.85596 (26)	0.34447 (34)	C(53)	0.39584 (29)	0.59280 (28)	0.50397 (35)
C(13)	0.41313 (29)	0.88146 (25)	0.31449 (33)	C(54)	0.48314 (29)	0.69316 (28)	0.37169 (36)
C(14)	0.48945 (29)	0.89992 (25)	0.40837 (34)	C(55)	0.45031 (33)	0.53225 (29)	0.29523 (39)
C(15)	0.58639 (30)	0.92806 (26)	0.41522 (33)	C(56)	0.33288 (31)	0.49680 (29)	0.40460 (39)
C(16)	0.66065 (29)	0.94483 (27)	0.50529 (35)	C(57)	0.36462 (28)	0.65811 (27)	0.48080 (36)
C(17)	0.76164 (28)	0.97676 (27)	0.50674 (34)	C(58)	0.34347 (31)	0.49929 (28)	0.29001 (37)
C(18)	0.81071 (27)	0.98506 (27)	0.60806 (33)	C(59)	0.37611 (31)	0.66020 (27)	0.36630 (36)
C(19)	0.73952 (28)	0.95849 (27)	0.66656 (33)	C(60)	0.31217 (30)	0.56509 (30)	0.26867 (36)
C(20)	0.76097 (28)	0.95939 (27)	0.77485 (35)	C(61)	0.63272 (29)	0.92429 (31)	1.09753 (35)
C(21)	0.82282 (28)	0.96996 (28)	1.02016 (34)	C(62)	0.13509 (31)	0.77570 (30)	0.63578 (38)
C(22)	0.88807 (30)	1.07131 (30)	1.08968 (35)	C(63)	0.42494 (31)	0.89051 (29)	0.20677 (38)
C(23)	0.99039 (29)	1.09887 (32)	1.14869 (34)	C(64)	0.91828 (31)	1.01974 (33)	0.65648 (40)
C(24)	1.14731 (33)	1.22586 (32)	1.25424 (41)	C(65)	0.87843 (37)	0.68655 (37)	0.35095 (51)
C(25)	1.19899 (32)	1.24433 (29)	1.17005 (38)	C(66)	0.38603 (69)	0.54414 (54)	0.95512 (82)

[a] Estimated standard deviations in the least significant figures are given in parentheses in this and all subsequent tables.

rification. The acid chloride in 20 mL of methylene chloride was placed under argon in one syringe of a two-syringe drive. In the other syringe was placed, under argon, a solution of 200 mg (0.28 mM) of 3,13-bis-(3-aminopropyl)-8,18-bis(2-carbobenzoxyethyl)-2,7,12,17-tetramethylporphyrin[27] and 1 mL of triethylamine in 19 mL of methylene chloride (see eq 1). These two solutions were injected at a rate of 1 mL/min per syringe at room temperature into 100 mL of degassed, dried methylene chloride, with magnetic stirring. After addition and 1 h of additional stirring, the solution was filtered and washed twice with 100 mL of water. The solution was dried and evaporated, and the product was purified by chromatography on silica gel with chloroform–methanol (100:1) elution. Crystallization from *n*-hexane–methylene chloride afforded 130 mg (53%) of crystalline product. Mass spectrum, parent peak 1020, calculated 1020 ($C_{64}H_{72}N_6O_6$). The NMR assignments are discussed below. All assignments of protons in the side chain and adamantane were made from decoupling experiments. NMR analysis of a solution from the crystals used for X-ray analysis showed 2 mol of methylene chloride (δ 5.28) per mol of product.

Adamantane–Hemin–6,6-Cyclophane Chloride (5^+Cl^-). Iron was inserted into adamantane–porphyrin–6,6-cyclophane (**5P**) by the standard ferrous sulfate procedure.[28] The product was chromatographed on silica gel with the dichloromethane–methanol (100:1) eluent and then crystallized from dichloromethane–*n*-hexane to yield fine needles (98%). This compound was converted to the iron(II) derivative for characterization as described below.

[Adamantane–Heme–6,6-Cyclophane]–1-Methylimidazole–Carbon Monoxide Complex (1-MeIm–5–CO). This compound was prepared in high concentration (~0.02 M) in chloroform solution or in low (μM) concentration in benzene by reduction with either aqueous or 18-crown-6 complexed sodium dithionite.[29] For NMR studies and crystallization, 10 mg of the hemin (5^+Cl^-) was placed in a serum-capped NMR tube flushed with carbon monoxide, and 0.5 mL of carbon monoxide saturated chloroform (or methylene chloride) was added by gastight syringe. First, 1 μL of 1-methylimidazole and then 0.3 mL of a saturated solution of sodium dithionite and carbon monoxide in D_2O were added and the tube was shaken vigorously until the solution became dark red. The tube was centrifuged and then the aqueous layer removed with a syringe. Visible spectra of a thin film on the walls of the tube showed conversion to the carbon monoxide complex. The 360-MHz NMR assignments of this complex are described below. Again, decoupling of all side-chain and adamantane protons aided in the assignments. Fine needles of the complex were obtained upon transferring the NMR sample under carbon monoxide into a diffusion cell and allowing *n*-hexane to condense into the chloroform.

Samples of the 1-MeIm–**5**–CO solution, prepared as described above, were transferred into matched infrared cells under carbon monoxide. Oxygen was added to one cell to oxidize the heme, and this cell was placed in the reference beam. A large peak at 1959 cm^{-1} characterized this difference spectrum.

Adamantane–Heme–Cyclophane–Bis(*tert*-butyl isocyanide) Complex [5–(*t*-BuNC)$_2$]. An approximately 0.05 M solution of the hemin (5^+Cl^-) in the presence of 0.1 M *tert*-butyl isocyanide was reduced under argon in an NMR tube as described above and the bis isocyanide complex was identified by its visible absorption spectrum. The NMR spectra, recorded at 21 and 6.2 °C, show several peaks that result from bound *tert*-butyl groups; there is hindered rotation about the isocyanide bond.

Titration of Adamantane–Heme–Cyclophane (5) with Ligands. The low affinity of this heme toward ligands allows direct titration. A 0.1-mL

(27) (a) Traylor, T. G.; Campbell, D.; Tsuchiya, S.; Koga, N.; Chang, C. K., in preparation. (b) Traylor, T. G.; Campbell, D.; Tsuchiya, S. *J. Am. Chem. Soc.* **1979**, *101*, 4748–4749.

(28) Falk, J. E. "The Porphyrins and Metalloporphyrins"; Elsevier: New York, 1964; p 133.

(29) Mincey, T.; Traylor, T. G. *Bioinorg. Chem.* **1978**, *9*, 409–420.

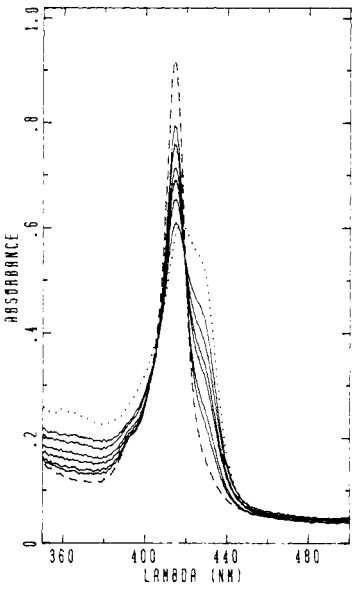

Figure 1. Titrations of **5**–DCIm in toluene with CO gas at 20 °C: (···) initial deoxy spectrum; (—) intermediate spectra at ([CO] × 10^{-6} M, torr) 1.57, 0.157; 3.13, 0.313; 4.70, 0.47; 6.27, 0.627; 11.5, 1.15; and 16.7, 1.67; (---) final CO spectrum at 1.21 × 10^{-4} M, 12.1 torr.

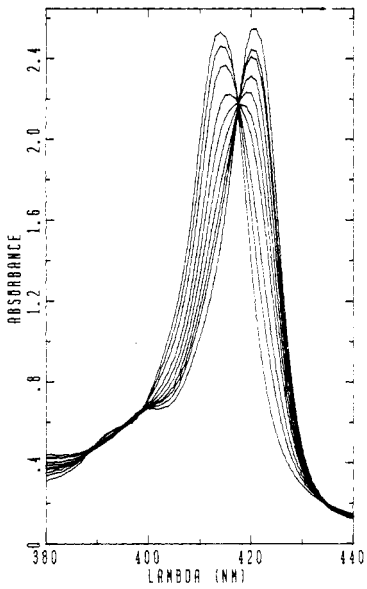

Figure 2. Displacement of CO from **5**–DCIm–CO by tosylmethyl isocyanide (TMIC) in toluene (0.1 M DCIm) at 23 °C. The CO partial pressure is 26.7 torr (2.67 × 10^{-4} M) and the increasing absorbance at 420 nm corresponds to the following concentrations of TMIC (× 10^4 M): 0.0, 0.50, 1.00, 2.00, 2.99, 4.48, 6.95, 11.9, and 16.7. Final spectrum obtained with [CO] ~ 0.0 and [TMIC] = 16.7 × 10^{-4} M.

solution of ~0.05 M adamantane–hemin–cyclophane chloride (5^+Cl^-) in chloroform was carefully degassed and treated with aqueous sodium dithionite. Approximately 5 μL of this solution was added, with an argon-flushed gastight syringe, to 3 mL of benzene or toluene containing 100 mg of either 1-methylimidazole, 100 mg of 1,5-dicyclohexylimidazole (DCIm)[7] (73 mg of DCIm when toluene was used), or no ligands in a 134-mL tonometer. To this argon-filled tonometer was added by gastight syringe aliquots of either carbon monoxide gas or neat isocyanides. After solutions were stirred at least 15 min to establish equilibria, spectra were taken. Careful argon flushing of the tonometer and solutions prevented oxidation. From a series of such spectra, exemplified by those in Figure 1, equilibrium constants were calculated. Isocyanide binding constants were determined by carbon monoxide displacements, illustrated in Figure 2.

Results

Description of the Structure. Monomeric units of adamantane–porphyrin–6,6-cyclophane (**5P**) crystallize as the bis(di-

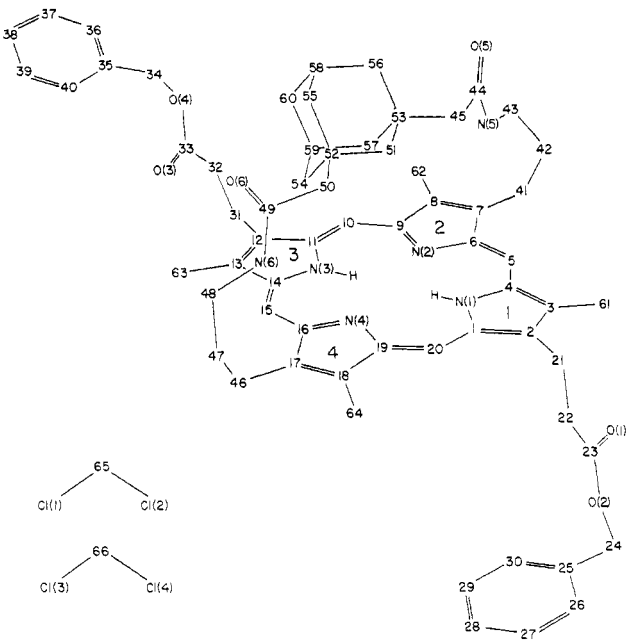

Figure 3. Atom-labeling scheme for 1,3-adamantane–3,13-porphyrin–6,6-cyclophane.

chloromethane) solvate. The molecular connectivity is as expected and is illustrated in Figure 3 along with the atom-numbering scheme. The crystal packing in one unit cell is illustrated in Figure 4. Molecules of **5P** stack in one-dimensional "chains" and are oriented so that the exposed sides of the porphyrin macrocycles overlap between neighboring molecules in a slipped-stack fashion with an interplanar spacing of 3.2 Å.[30] In addition, the "strapped" sides of the porphyrins are interlocked between neighboring intrachain molecules. The CH_2Cl_2 solvent molecules occupy sites near the "straps" and are involved in some short intrachain van der Waals' type contacts with the oxygen atoms of the amide groups (H1(C65)···O(5) = 2.30 Å and H2(C66)···O(6) = 2.45 Å). There are no unusual intermolecular contacts of the solvent–solvent or porphyrin–porphyrin type. This molecular arrangement is in contrast to the packing found in the solid-state structures of the model compounds $H_2(C_2\text{-Cap})\cdot 5CHCl_3\cdot CH_3OH$[31] and $FeCl(C_2\text{-Cap})\cdot 3CHCl_3$[32] where the porphyrin molecules are immersed in matrices of solvent molecules. This difference in crystal packing may account for the crystal stability of **5P** relative to the C_2-Cap compounds, both of which rapidly desolvate at room temperature.

As can be seen in Figure 5, compound **5P** is a β-carbon-substituted, free-base porphyrin in which opposite pairs of pyrrole rings are substituted in the same manner. Pyrrole rings 2 and 4 each have a methyl substituent in addition to being bridged by an adamantane-1,3-[6(2-oxo-3-aza,6(2-oxo-3-aza)] substituent while pyrrole rings 1 and 3 are each substituted by a methyl group and a nonbridging carbobenzoxyethyl group. From a difference electron density calculation the imino hydrogen atoms were easily identified as being bonded to pyrrole rings 1 and 3.

Selected distances and angles are listed in Tables VI and VII. Chemically equivalent bond lengths and angles of the porphyrin macrocycle are equal within experimental error and compare favorably with other free-base porphyrins.[33] The 24-atom porphyrin skeleton is essentially planar (Table VIII[26] and Figure 6), with the mean displacement from the least-squares plane being 0.038 Å and the maximum displacement being 0.101 (4) Å for atom C(8). The small dihedral angle (3.2°) between the two

(30) We define the interplanar spacing to be the distance between the centroid of the four porphyrin nitrogen atoms and the best least-squares plane of the neighboring 24-atom porphyrin macrocycle.
(31) Jameson, G. B.; Ibers, J. A. *J. Am. Chem. Soc.* **1980**, *102*, 2823–2831.
(32) Sabat, M.; Ibers, J. A. *J. Am. Chem. Soc.* **1982**, *104*, 3715–3721.
(33) See Table XII of ref 31.

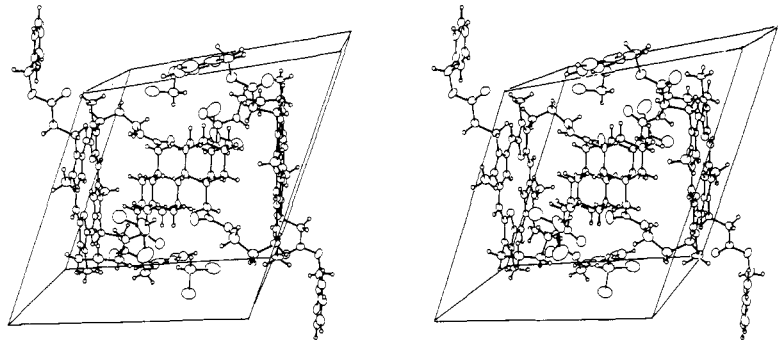

Figure 4. Stereoscopic packing diagram viewed down the *c* axis. Probability ellipsoids are drawn at the 50% level except for hydrogen atoms, which have been drawn artificially small.

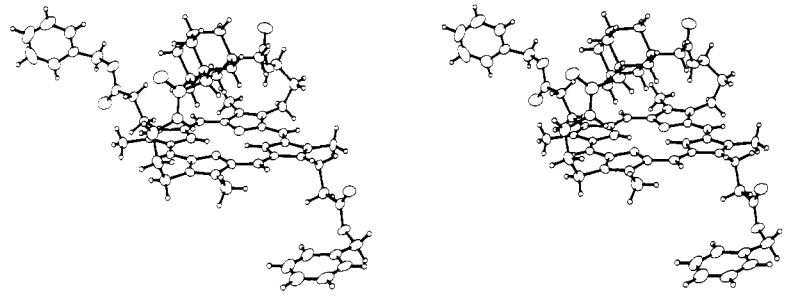

Figure 5. Stereodiagram of 1,3-adamantane-3,13-porphyrin-6,6-cyclophane (**5P**).

"strapped" pyrrole rings along with the small displacements from planarity suggest that the adamantane bridge imposes little steric strain upon the porphyrin macrocycle. This is in contrast with the dihedral angle of 112° between bridged pyrrole rings in 7,17-diethyl-2,8,12,18-tetramethyl-3,13-nonamethyleneporphyrin,[34] where a 9-atom strap imposes considerable steric strain upon the porphyrin ring.

The metrical parameters of the porphyrin substituents are not unusual. The carbobenzoxyethyl side chains are oriented on opposite sides of the porphyrin ring and show good agreement between chemically equivalent bond distances and angles. Although the adamantane bridge is in an offset orientation relative to the plane of the porphyrin, the conformations of the two linking chains (atoms C(41)···C(45) and C(46)···C(50)) are very similar, as evidenced by chemically equivalent torsion angles being comparable in magnitude (Table IX[26]). Within the two linking chains, bond angles having an sp^3 carbon atom at the apex tend to deviate more from idealized tetrahedral geometry (mean = 114.6 (21)°; range = 111.5 (4)–118.1 (4)°) than similar bond angles in the nonbridging side chains (mean = 112.5 (10)°; range = 112.6 (4)–114 (3)°). This may indicate that steric strain imposed by the adamantane bridge is being relieved through bond angle distortion in the side chains.

The gross structure of **5P** is most readily comparable with the structures of anthracene- and pyridine-bridged porphyrins reported recently.[35] In all three examples bridging atoms are in relatively close contact with atoms of the porphyrin macrocycle and so no effective void between the porphyrin and the strap remains. But in contrast to the anthracene- and pyridine-bridged porphyrins, porphyrin **5P** has a bulky, nonaromatic, bridging group (adamantane) and consequently it also has close intramolecular contacts between alkyl hydrogen atoms and the porphyrin macrocycle. Adamantane hydrogen atoms are calculated to be as close as 2.5 Å (H1(C54)) to the plane of the porphyrin, and the shortest contact between a strap hydrogen atom and the centroid of the four porphyrin nitrogen atoms is 2.7 Å for atom H2(C57).

Nuclear Magnetic Resonance Studies. NMR assignments of the porphyrin **5P** in chloroform are given in Figure 7. The first

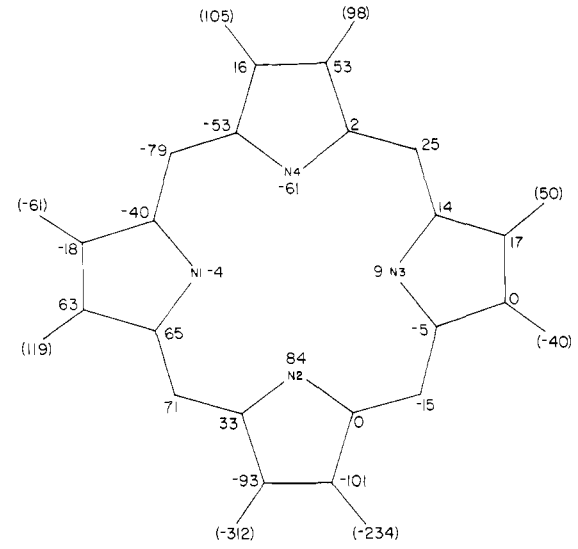

Figure 6. Displacements (in Å × 10^3) of atoms from the least-squares plane of the 24-atom porphyrin skeleton. The estimated standard deviations are 0.004 Å for nitrogen atoms and 0.004–0.005 Å for carbon atoms. Displacements in parentheses were not included in the calculation of the least-squares plane.

striking effect is that the asymmetry of the molecule has caused different shielding of the strap and adamantane–porphyrin above the four quadrants (pyrrole areas) of the porphyrin (see Figure 8). Thus the geminal protons are potentially diastereotopic. The symmetry of the porphyrin causes the area above the pyrrole groups labeled *R* and *R'* to have similar shielding and above *S* and *S'* to have similar shielding. Thus the propylamine protons are split by this asymmetry, 3.19, 3.44 and 3.96, 4.30. If the adamantane prefers the indicated position close to the porphyrin but flips rapidly between two equal positions, then the shielding of proton A near *S* in one conformation is equivalent to that of A' near *S'* in the other and the same relationship holds for proton B near *R* vs. proton B' near *R'*. This results in an A-type CH_2 group in which one proton points axially toward the porphyrin plane and the other is farther away in an equatorial position. This gives doublets (J = 12 Hz) at −3.02 and −0.76 for axial and

(34) Einstein, F. W. B.; Jones, T. Twelfth International Congress of Crystallography **1981**, 09.2-34, Abstract C212.

(35) Cruse, W. B.; Kennard, O.; Sheldrick, G. M.; Hamilton, A. D.; Hartley, S. G.; Battersby, A. R. *J. Chem. Soc. D* **1980**, 700–701.

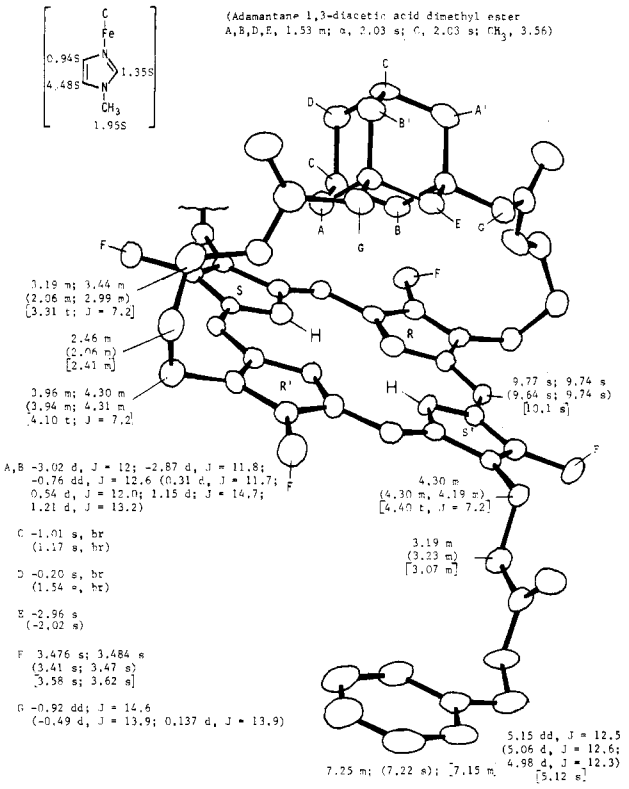

Figure 7. Nuclear magnetic resonance assignments of adamantane–porphyrin–6,6-cyclophane (**5P**), adamantane–heme–6,6-cyclophane–1-MeIm–CO complex (MeIm–**5**–CO) (in parentheses), and the precursor porphyrin (strap replaced with two $(CH_2)_3NH_2$ groups) in chloroform (in brackets). Insets give free adamantane and bound imidazole assignments. Chemical shifts are in ppm downfield from Me_4Si.

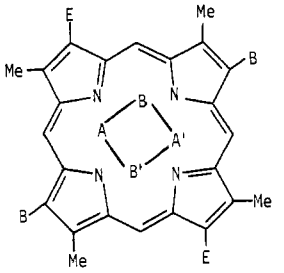

Figure 8. Symmetry relationships of the methylene groups labeled A, A′, B, and B′ in Figure 7 as the adamantane adopts the left (unprimed (CH_2)s down) conformation or the right (primed (CH_2)s down) conformation. The side chains are carbobenzoxyyethyl (E) and cyclophane bridge (B).

equatorial A protons. The β protons would then be the doublets (J = 12 Hz) at −2.87 and −0.76. Notice that because of the conformational interchange, only one kind of propionic acid proton set is observed as well as one kind of C, D, and E protons.

The NMR assignment of 1-methylimidazole–**5**–carbon monoxide (MeIm–**5**–CO) is given in parentheses in Figure 7 and both can be compared with the precursor porphyrin (in brackets) and adamantane structures (inset) in the same figure. The adamantane protons are shifted much farther upfield in the porphyrin than in the heme complex, indicating a reduction of ring current upon incorporation of the iron(II). The CO complex displays two sets of carbobenzoxyethyl protons as well as the protons α to the amide carbonyl groups. These latter protons display greater splitting than those in the parent, indicating possible alteration in conformation or increased asymmetry of the CO complex.

The bis(*tert*-butyl isocyanide) complex, **5**–(*t*-BuNC)$_2$, displays a single peak for one bound *tert*-butyl isocyanide group and multiple peaks for the other. These multiple peaks can be attributed to a slowly rotating *tert*-butyl group and a slowly interconverting adamantane group. Molecular models indicate that flipping of the adamantane group across the bound ligand should be prevented in the isocyanide complex and retarded in the CO complex.

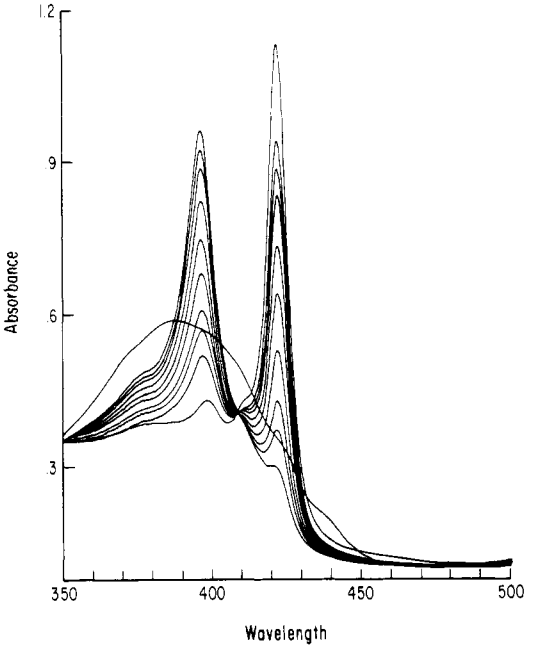

Figure 9. Titration of **5** with TMIC in benzene at 23 °C. The broad band at 389 nm corresponds to [TMIC] = 0.0, while the increasing absorbance at 423 nm corresponds to [TMIC] ($\times 10^5$ M) of 1.3, 2.6, 5.85, 12.4, 18.9, 25.4, 38.4, 51.4, 83.9, and 1.9×10^{-2}.

Spectroscopic Properties. The UV–visible spectra of **5**P and some of the iron derivatives are shown in Table X. Compared with the mesoporphyrin derivatives, which should be electronically similar, the Soret bands of the adamantane–cyclophane–**5** derivatives are red-shifted by 2 or 3 nm. A similar shift was seen in the anthracene–heme–6,6-cyclophane derivatives.

Titration of 5 with Ligands. The use of 1,5-dicyclohexylimidazole (DCIm) as proximal base in heme–cyclophanes has served to prevent binding of a second base in several systems.[5,7,9] In fact, the formation of five-coordinated heme with DCIm can be taken as strong evidence for a cyclophane rather than an open structure and constitutes a useful method for structure proof on small quantities of synthetic materials thought to be cyclophanes. At 1 M DCIm no evidence for hexacoordination in **5** was observed. Although we did not accurately titrate **5** with 1-methylimidazole, we observed that a solution of **5** in pure 1-MeIm was not completely converted to the hexacoordinated form ($K_B^B \cong 1$ M^{-1}).

The affinity of **5** for DCIm was determined by direct titration. A reduced solution of **5** in toluene, in the presence of a small volume of aqueous sodium dithionite, was titrated with a toluene solution of DCIm under argon. The titration curve showed a Hill slope, n = 0.92, and a binding constant, $K^B = 6.0 \times$ M^{-1}. This titration is made somewhat inaccurate by the presence of the aqueous layer and by the partial binding of water to the five-coordinated product, indicated by some absorbance at 417 nm compared with 427 nm for the pure five-coordinated species.

The binding of carbon monoxide to five-coordinated **5**–B (B = MeIm or DCIm) was determined by direct titration with CO gas in a tonometer, as shown in Figure 1. Titrations in benzene containing 0.1 M 1-methylimidazole at 21 °C gave $K_B^{CO} = 1.6 \times 10^5$ M^{-1} (1.60 torr^{-1}) whereas in 0.1 M DCIm solution values of 1.2×10^5 M^{-1} (1.20 torr^{-1}) and 1.4×10^5 M^{-1} (1.40 torr^{-1}) were obtained. The value in toluene containing 0.1 M DCIm was 1.74×10^5 M^{-1} (1.74 torr^{-1}) at 20 °C.

Isocyanide binding constants to **5**–DCIm in benzene at 23 °C were determined by RNC displacement with CO, as illustrated in Figure 2. Displacement constants, ($K_{DCIm}^{RNC,CO}$) were 4.1 for *t*-BuNC and 0.6 for *p*-tosylmethyl isocyanide (TMIC), which gives values of $K_{DCIm}^{t\text{-BuNC}} = 3 \times 10^4$ M^{-1} and $K_{DCIm}^{TMIC} = 2 \times 10^5$

Table VI. Selected Bond Distances (Å) for 1,3-Adamantane-3,13-Porphyrin-6,6-Cyclophane

atoms	separation	av[a]	atoms	separation	av
N(1)-C(1)	1.374 (6)		C(5)-C(4)	1.386 (6)	
N(1)-C(4)	1.366 (5)		C(5)-C(6)	1.399 (6)	
N(2)-C(6)	1.365 (5)		C(10)-C(9)	1.405 (6)	
N(2)-C(9)	1.362 (5)	$N-C_a$[b] = 1.364 (6)	C(10)-C(11)	1.367 (6)	C_a-C_m = 1.388 (6)
N(3)-C(11)	1.367 (5)		C(15)-C(14)	1.387 (6)	
N(3)-C(14)	1.360 (5)		C(15)-C(16)	1.393 (6)	
N(4)-C(16)	1.358 (6)		C(20)-C(19)	1.392 (6)	
N(4)-C(19)	1.365 (5)		C(20)-C(1)	1.375 (6)	
C(1)-C(2)	1.431 (6)		C(2)-C(21)	1.496 (6)	1.496 (6)
C(4)-C(3)	1.432 (6)	C_a-C_b = 1.432 (6)	C(12)-C(31)	1.497 (6)	
C(11)-C(12)	1.433 (6)		C(21)-C(22)	1.502 (6)	1.506 (6)
C(14)-C(13)	1.434 (6)		C(31)-C(32)	1.510 (6)	
C(6)-C(7)	1.463 (6)		C(22)-C(23)	1.488 (6)	1.492 (6)
C(9)-C(8)	1.451 (5)	1.456 (6)	C(32)-C(33)	1.497 (6)	
C(16)-C(17)	1.459 (6)		C(23)-O(1)	1.209 (5)	1.202 (13)
C(19)-C(18)	1.453 (5)		C(33)-O(3)	1.191 (6)	
C(2)-C(3)	1.369 (6)	C_b-C_b = 1.363 (9)	C(23)-O(2)	1.332 (6)	1.334 (6)
C(7)-C(8)	1.357 (6)		C(33)-O(4)	1.337 (6)	
C(12)-C(13)	1.351 (6)	1.355 (6)	O(2)-C(24)	1.431 (6)	1.445 (20)
C(17)-C(18)	1.360 (6)		O(4)-C(34)	1.459 (6)	
C(25)-C(26)	1.380 (7)		C(24)-C(25)	1.496 (7)	1.489 (9)
C(26)-C(27)	1.382 (7)		C(34)-C(35)	1.483 (7)	
C(27)-C(28)	1.382 (7)	1.387 (7)	N(5)-C(44)	1.330 (6)	1.336 (9)
C(28)-C(29)	1.393 (7)		N(6)-C(49)	1.343 (6)	
C(29)-C(30)	1.386 (7)		O(5)-C(44)	1.224 (6)	1.217 (11)
C(30)-C(25)	1.397 (7)		O(6)-C(49)	1.209 (6)	
C(35)-C(36)	1.368 (7)		C(44)-C(45)	1.495 (7)	1.504 (13)
C(36)-C(37)	1.341 (8)		C(49)-C(50)	1.513 (7)	
C(37)-C(38)	1.342 (10)		C(45)-C(53)	1.534 (7)	1.545 (13)
C(38)-C(39)	1.390 (10)	1.364 (20)	C(50)-C(52)	1.555 (7)	
C(39)-C(40)	1.377 (9)		C(51)-C(52)	1.529 (7)	
C(40)-C(35)	1.366 (7)		C(51)-C(53)	1.539 (6)	
C(7)-C(41)	1.490 (6)	1.496 (8)	C(52)-C(54)	1.520 (6)	
C(17)-C(46)	1.501 (6)		C(52)-C(55)	1.517 (6)	
C(41)-C(42)	1.532 (7)	1.520 (16)	C(53)-C(56)	1.531 (6)	
C(46)-C(47)	1.509 (7)		C(53)-C(57)	1.532 (6)	
C(42)-C(43)	1.513 (7)	1.507 (9)	C(54)-C(59)	1.534 (6)	1.528 (7)
C(47)-C(48)	1.501 (7)		C(55)-C(58)	1.532 (7)	
C(43)-N(5)	1.454 (6)	1.458 (6)	C(56)-C(58)	1.532 (7)	
C(48)-N(6)	1.462 (6)		C(57)-C(59)	1.532 (7)	
C(3)-C(61)	1.482 (6)		C(58)-C(60)	1.532 (6)	
C(8)-C(62)	1.500 (6)	1.494 (11)	C(59)-C(60)	1.515 (6)	
C(13)-C(63)	1.487 (6)				
C(18)-C(64)	1.506 (6)				
C(65)-Cl(1)	1.744 (7)				
C(65)-Cl(2)	1.755 (5)				
C(66)-Cl(3)	1.775 (10)				
C(66)-Cl(4)	1.648 (9)				

[a] Here, and elsewhere, the estimated standard deviation given in parentheses following a mean value is the larger of that calculated for an individual observation on the assumption that the values averaged are from the same population or of that calculated for an individual parameter from the inverse of the least-squares matrix. [b] The nomenclature is that of: Hoard, J. L. *Science (Washington, D. C.)* **1971**, *174*, 1295-1302.

M^{-1}, respectively. Titration of **5** with isocyanides to determine K_{RNC}^{RNC} was carried out by adding a small amount of isocyanide to produce **5**–RNC and then titrating with additional aliquots on RNC. A typical set of titration curves is shown in Figure 9.

Kinetics of Dioxygen and Carbon Monoxide Reactions with Adamantane–Heme–Cyclophane (5)–DCIm. The rate of reaction of CO with **5** in toluene at 20 ± 0.1 °C was determined as a function of DCIm concentration. The data are summarized in Table XI. The rate becomes constant at (9.2 ± 0.2) × 10^3 M^{-1} s^{-1} above 0.4 M.

Dioxygen reaction with **5**–DCIm was studied by flashing CO from a 3-mL toluene solution of **5** that contained 0.45 M DCIm and a constant pressure of CO and varying O_2 pressures in a 134-mL tonometer as previously described.[20] From time-resolved spectra it is known that such a process proceeds first to partial or complete formation of the dioxygen complex followed by a slower return to the CO complex.[20a,36a] The fast process is represented by eq 2 in which conditions can be chosen so that

$$k_{obsd}^{fast} = k_B^{O_2}[O_2] + k^{-O_2} + k_B^{CO}[CO] \quad (2)$$

$k_B^{CO}[CO]$ is negligible. Plots of k_{obsd}^{fast} vs. dioxygen partial pressure at constant CO pressure are shown in Figure 10. These two plots afford $k_B^{O_2}$ = (1.5 ± 0.2) × 10^5 and (1.48 ± 0.2) × 10^5 M^{-1} s^{-1} and k^{-O_2} = 700 ± 75 and 670 ± 85 s^{-1}.

The slow process, under all conditions, is given by k^{-O_2} times the fraction returning to the CO complex. We prefer to determine first the rate without dioxygen ($k_B^{CO}[CO]$) and, leaving [CO]

(36) (a) Lavalette, D.; Momenteau, M. *J. Chem. Soc., Perkin Trans. 2* **1982**, 385–388. (b) Momenteau, M.; Lavalette, D. *J. Chem. Soc., Chem. Commun.* **1982**, 341–343.

Table VII. Selected Bond Angles (deg) for 1,3-Adamantane-3,13-Porphyrin-6,6-Cyclophane

atoms	angle	av
C(1)-N(1)-C(4)	110.0 (3)	C_a-N-C = 110.0 (3)
C(11)-N(3)-C(14)	110.1 (3)	
C(6)-N(2)-C(9)	104.7 (3)	105.0 (5)
C(16)-N(4)-C(19)'	105.4 (3)	
N(1)-C(1)-C(2)	106.8 (3)	N-C_a-C_b = 106.9 (8)
N(1)-C(4)-C(3)	107.6 (4)	
N(3)-C(11)-C(12)	106.1 (3)	
N(3)-C(14)-C(13)	107.8 (4)	
N(2)-C(6)-C(7)	112.1 (3)	111.6 (5)
N(2)-C(9)-C(8)	111.3 (4)	
N(4)-C(16)-C(17)	111.5 (3)	
N(4)-C(19)-C(18)	111.0 (4)	
C(1)-C(2)-C(3)	108.3 (4)	C_a-C_b-C_b = 108.1 (11)
C(2)-C(3)-C(4)	107.3 (4)	
C(11)-C(12)-C(13)	109.2 (3)	
C(12)-C(13)-C(14)	106.7 (4)	
C(6)-C(7)-C(8)	104.8 (4)	106.0 (10)
C(7)-C(8)-C(9)	107.2 (4)	
C(16)-C(17)-C(18)	105.6 (4)	
C(17)-C(18)-C(19)	106.5 (4)	
C(1)-C(2)-C(21)	124.3 (4)	C_a-C_b-C = 125.0 (9)
C(11)-C(12)-C(31)	125.6 (4)	
C(6)-C(7)-C(41)	127.0 (4)	127.2 (4)
C(16)-C(17)-C(46)	127.4 (4)	
C(4)-C(3)-C(61)	125.1 (4)	125.0 (5)
C(14)-C(13)-C(63)	125.5 (4)	
C(9)-C(8)-C(62)	124.3 (4)	
C(19)-C(18)-C(64)	125.2 (4)	
C(3)-C(2)-C(21)	127.4 (4)	C_b-C_b-C_β = 126.3 (6)
C(13)-C(12)-C(31)	125.1 (4)	
C(8)-C(7)-C(41)	128.0 (4)	127.5 (8)
C(18)-C(17)-C(46)	126.9 (4)	
C(2)-C(3)-C(61)	127.6 (4)	128.0 (4)
C(12)-C(13)-C(63)	127.8 (4)	
C(7)-C(8)-C(62)	128.5 (4)	
C(17)-C(18)-C(64)	128.2 (4)	
C(2)-C(21)-C(22)	112.3 (3)	111.8 (6)
C(12)-C(31)-C(32)	111.4 (3)	
C(21)-C(22)-C(23)	114.5 (4)	113.6 (13)
C(31)-C(32)-C(33)	112.7 (4)	
C(22)-C(23)-O(1)	125.0 (4)	125.7 (9)
C(32)-C(33)-O(3)	126.3 (4)	
C(7)-C(41)-C(42)	115.4 (4)	115.1 (4)
C(17)-C(46)-C(47)	114.8 (4)	
C(41)-C(42)-C(43)	114.9 (4)	115.5 (8)
C(46)-C(47)-C(48)	116.1 (4)	
C(42)-C(43)-N(5)	111.5 (4)	111.9 (6)
C(47)-C(48)-N(6)	112.3 (4)	
C(43)-N(5)-C(44)	124.9 (4)	123.8 (12)
C(48)-N(6)-C(49)	122.6 (4)	
N(5)-C(44)-O(5)	121.8 (4)	121.8 (5)
N(6)-C(49)-O(6)	121.9 (5)	
N(5)-C(44)-C(45)	115.3 (4)	114.8 (8)
N(6)-C(49)-C(50)	114.2 (4)	
O(5)-C(44)-C(45)	122.9 (4)	123.3 (6)
O(6)-C(49)-C(50)	123.8 (5)	
C(44)-C(45)-C(53)	118.1 (4)	115.9 (31)
C(49)-C(50)-C(52)	113.6 (4)	
C(45)-C(53)-C(51)	107.0 (3)	106.9 (3)
C(50)-C(52)-C(51)	106.8 (3)	
C(45)-C(53)-C(57)	111.8 (3)	111.5 (6)
C(50)-C(52)-C(54)'	110.9 (4)	

atoms	angle	av
N(1)-C(1)-C(20)	125.6 (4)	N-C_a-C_m = 125.2 (4)
N(1)-C(4)-C(5)	124.8 (4)	
N(3)-C(11)-C(10)	124.9 (4)	
N(3)-C(14)-C(15)	125.3 (4)	
N(2)-C(6)-C(5)	123.6 (4)	124.3 (5)
N(2)-C(9)-C(10)	124.3 (4)	
N(4)-C(16)-C(15)	124.9 (4)	
N(4)-C(19)-C(20)	124.4 (4)	
C(2)-C(1)-C(20)	127.6 (4)	C_b-C_a-C_m = 127.7 (9)
C(3)-C(4)-C(5)	127.5 (4)	
C(12)-C(11)-C(10)	128.9 (4)	
C(13)-C(14)--C(15)	126.8 (4)	
C(7)-C(6)-C(5)	124.3 (4)	124.2 (4)
C(8)-C(9)-C(10)	124.4 (4)	
C(17)-C(16)-C(15)	123.6 (4)	
C(18)-C(19)-C(20)	124.6 (4)	
C(4)-C(5)-C(6)	127.8 (4)	C_a-C_m-C_a = 127.5 (4)
C(14)-C(15)-C(16)	127.2 (4)	
C(9)-C(10)-C(11)	128.9 (4)	128.6 (5)
C(19)-C(20)-C(1)	128.2 (4)	
C(22)-C(23)-O(2)	111.5 (4)	110.9 (9)
C(32)-C(33)-O(4)	110.2 (4)	
O(1)-C(23)-O(2)	123.5 (4)	123.5 (4)
O(3)-C(33)-O(4)	123.5 (4)	
C(23)-O(2)-C(24)	117.0 (4)	117.0 (4)
C(33)-O(4)-C(34)	116.9 (4)	
O(2)-C(24)-C(25)	112.6 (4)	112.6 (4)
O(4)-C(34)-C(35)	112.6 (4)	
C(24)-C(25)-C(26)	119.5 (4)	120.7 (14)
C(24)-C(25)-C(30)	122.0 (4)	
C(34)-C(35)-C(36)	119.4 (5)	
C(34)-C(35)-C(40)	121.9 (5)	
C(25)-C(26)-C(27)	121.9 (5)	120.0 (12)
C(26)-C(27)--C(28)	119.1 (5)	
C(27)-C(28)-C(29)	120.3 (5)	
C(28)-C(29)-C(30)	119.6 (5)	
C(29)-C(30)-C(25)	120.5 (5)	
C(30)-C(25)-C(26)	118.4 (5)	
C(35)-C(36)-C(37)	121.9 (5)	120.0 (12)
C(36)-C(37)-C(38)	120.2 (6)	
C(37)-C(38)-C(39)	120.0 (6)	
C(38)-C(39)-C(40)	119.0 (5)	
C(39)-C(40)-C(35)	120.3 (5)	
C(40)-C(35)-C(36)	118.3 (5)	
C(51)-C(52)-C(54)	108.3 (3)	109.5 (9)
C(51)-C(52)-C(55)	109.0 (4)	
C(51)-C(53)-C(56)	108.3 (3)	
C(51)-C(53)-C(57)	107.8 (3)	
C(52)-C(51)-C(53)	111.7 (3)	
C(52)-C(54)-C(59)	109.6 (4)	
C(52)-C(55)-C(58)	110.1 (4)	
C(53)-C(56)-C(58)	110.0 (4)	
C(53)-C(57)-C(59)	110.2 (3)	
C(54)-C(59)-C(57)	109.7 (3)	
C(54)-C(59)-C(60)	109.8 (4)	
C(55)-C(58)-C(56)	109.3 (4)	
C(55)-C(58)-C(60)	109.2 (4)	
C(56)-C(58)-C(60)	110.0 (3)	
C(57)-C(59)-C(60)	109.4 (4)	
C(58)-C(60)-C(59)	109.3 (3)	
Cl(1)-C(65)-Cl(2)	110.9 (3)	
Cl(3)-C(66)-Cl(4)	113.3 (4)	

Table X. Electronic Spectra of Adamantane–Porphyrin–6,6-Cyclophane Derivatives[a]

compd	solvent	λ (ε × 10^{-3} M^{-1} cm^{-1})
porphyrin	$CHCl_3$	622, 568, 535, 500, 401, 379 sh
hemin	benzene	630 (4.7), 532 (8.1), 504 (7.4), 402 sh (59), 375 (76)
heme–DCIm	toluene	550 (10), 427 (96)
heme–DCIm–CO	toluene	554 (11), 534 (11), 413 (220)
heme–1-MeIm–CO	benzene	553 (9.5), 533 (10), 413 (220)
heme–1,2-Me_2Im	benzene	548 (11), 427 (120)
heme–1,2-Me_2Im–CO	benzene	540 (13), 412 (210)
heme–*t*-BuNC	benzene	540 (12), 425 (55), 412 (49), 398 (77)
heme–(*t*-BuNC)$_2$	benzene	553 (10), 525 (8.5), 425 (160), 402 (44)
heme–*t*-BuNC–1-MeIm	benzene	552 (22), 522 (16), 423 (190)
heme–*n*-BuNC	benzene	559, 541, 423, 410 sh, 398
heme–(*n*-BuNC)$_2$	benzene	554, 526, 425

[a] Base concentration 0.1–0.8 M.

Table XI. Rates of CO Recombination after Flash Photolysis of **5**–DCIm in Toluene at 20.0 ± 0.1 °C[a]

[DCIm], M	[CO], M × 10^3	k_{obsd}/[CO], M^{-1} s^{-1} × 10^{-3}
0.0097	1.64	37.1
0.0323	1.64	22.2
0.072	1.64	15.5
0.105	1.64	13.3
0.251	1.27	10.0
0.40	1.15	8.89
0.51	1.10	9.13
0.62	1.12	9.17
0.70	1.11	9.05
0.82	1.10	9.54

[a] Solubility of CO, 1 × 10^{-5} M $torr^{-1}$.[21a]

the same, plot the rates as a function of $[O_2]$ by the completely general equation.[20b]

$$\frac{k_B^{CO}[CO]}{k_{obsd}^{slow}} = \frac{k_B^{CO}[CO]}{k_B^{-O_2}} + K_B^{O_2}[O_2] + 1 + \frac{k_B^{-CO}}{k_B^{-O_2}} \quad (3)$$

Four such plots are shown in Figure 11. The values for $K_B^{O_2}$ = 310 ± 18, 246 ± 16, 263 ± 23, and 262 ± 27 yield an average value of $K_B^{O_2}$ = 270 ± 24 M^{-1} (0.0033 $torr^{-1}$). The intercepts are near 1 and therefore dissociation rates cannot be obtained from this plot. However, division of the slope of Figure 10 by that of Figure 11 gives $k_B^{O_2}/K_B^{O_2} = k_B^{-O_2}$ = 540 s^{-1}, in reasonable agreement with the intercept of eq 2.

Discussion

Influence of Factors Other Than Distal-Side Steric Effects on Ligation. The design of molecules that incorporate steric effects to iron ligation involves the synthesis of cyclophanes in which other factors affecting ligation can be changed. Therefore, in order to draw inferences concerning the nature of steric effects, these other influences must be shown to be absent or must be quantitatively determined.

Both O_2 binding and CO binding are sensitive to porphyrin deformation such as occurs in the change from R- to T-state in hemoglobin or T-state model compounds.[14,18,37] The crystal structure of **5P** demonstrates that the adamantane–cyclophane–porphyrin has the same flat geometry as do non-cyclophane–porphyrins. We have shown that enforced porphyrin doming retards the CO association rate and increases the CO dissociation rate.[14] The similarity of k_B^{-CO} in the adamantane– and anthracene–cyclophanes to that of open model compounds is further evidence against such deformation.

It has been suggested that amide functions in the cyclophane straps or in tetrakis(*o*-pivalamidophenyl)heme[17a] increase the local polarity, which increases dioxygen affinity.[36b] Solvent polarity effects cause $k_B^{-O_2}$ to decrease.[17b,38] Although adamantane–heme

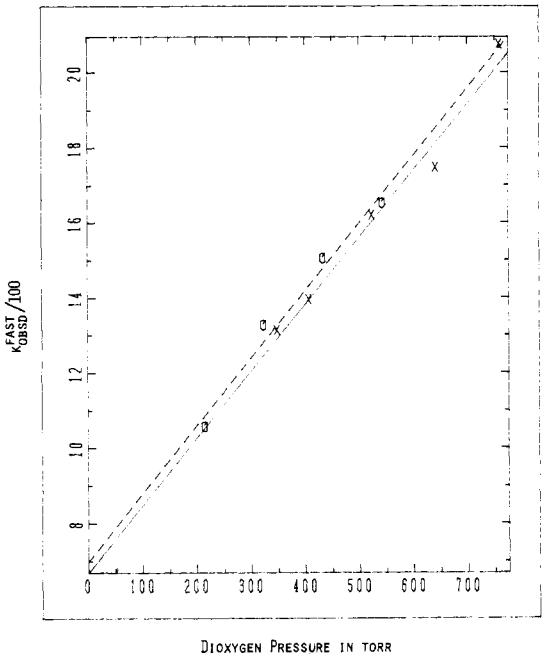

Figure 10. Plots of k_{obsd}^{fast} (after flash photolysis of DCIm–**5**–CO) vs. dioxygen partial pressure over toluene (0.45 M DCIm) at 20 °C: (O) [CO] = 1.09 mM, 109 torr, slope = 1.50 × 10^5 M^{-1} s^{-1}; (×) [CO] = 1.17 mM, 117 torr, slope = 1.48 × 10^5 M^{-1} s^{-1}.

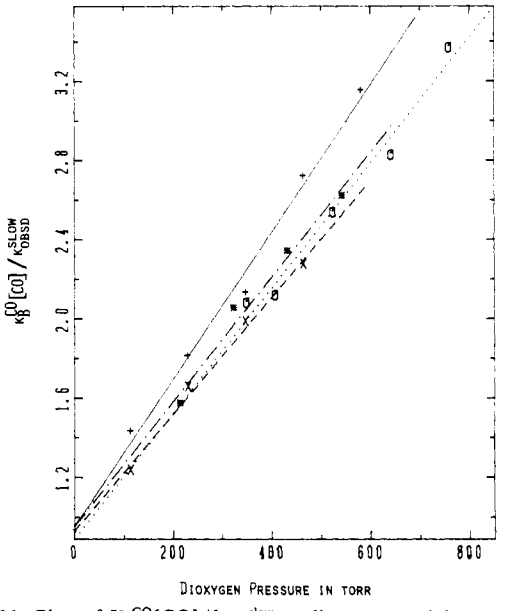

Figure 11. Plots of $K_B^{CO}[CO]/k_{obsd}^{slow}$ vs. dioxygen partial pressure over toluene (0.45 M DCIm) at 20 °C: (+) [CO] = 1.75 mM, 175 torr, $k_B^{CO}[CO]$ = 19.5 s^{-1}, slope = 3.72 × 10^{-3} $torr^{-1}$; (×) [CO] = 1.76 mM, 176 torr, $k_B^{CO}[CO]$ = 18.2 s^{-1}, slope = 2.95 × 10^{-3} $torr^{-1}$; (O) [CO] = 1.17 mM, 117 torr, $k_B^{CO}[CO]$ = 12.5 s^{-1}, slope = 3.16 × 10^{-3} $torr^{-1}$; (*) [CO] = 1.09 mM, 109 torr, $k_B^{CO}[CO]$ = 11.0 s^{-1}, slope = 3.15 × 10^{-3} $torr^{-1}$.

5 and anthracene–6,6- and –7,7-cyclophanes **1a** and **1b** all show a 5–7-fold reduction in $k_B^{-O_2}$, all three have similar dioxygen dissociation rates. This suggests that the 7,7-cyclophane, which shows little or no steric hindrance toward CO binding, and the adamantane–heme, which displays a 1000-fold reduction in CO affinity, have similar polarities around their binding sites.

An additional problem that plagues sterically hindered hemes is the increased tendency toward the base-elimination mechanism.[7] This could easily lead to inaccurate kinetic results. However, as seen in Table XI, the CO association rate becomes independent

(37) Collman, J. P.; Brauman, J. I.; Doxsee, K. M.; Halbert, T. R.; Suslick, K. S. *Proc. Natl. Acad. Sci. U.S.A.* **1978**, *75*, 564–568.

(38) Traylor, T. G.; White, D. K.; Campbell, D. H.; Berzinis, A. P. *J. Am. Chem. Soc.* **1981**, *103*, 4932–4936.

Table XII. Rate Constants for Reaction of Hemes and Hemoproteins with Dioxygen and Carbon Monoxide[a]

compd	solvent	k_B^{CO}, M^{-1} s^{-1}	k_B^{-CO}, s^{-1}	$k_B^{O_2}$, M^{-1} s^{-1}	$k_B^{-O_2}$, s^{-1}	$P_{1/2}^{O_2}$, torr	$P_{1/2}^{CO}$, torr	$M = P_{1/2}^{O_2}/P_{1/2}^{CO}$	ref
myoglobin	H_2O	5×10^5	0.02	1.5×10^7	11	0.42	0.024	17	*b*
Hb(R)	H_2O	6×10^6	0.009	6×10^7	12–21	0.16	0.001	2×10^2	*c*
chelated protoheme	H_2O/MTAB	3.6×10^6	0.009	2.6×10^7	47	1.0	0.002	5×10^2	*d*
	benzene	1.1×10^7	0.025	6.2×10^7	4×10^3	5.6	2.5×10^{-4}	2.2×10^4	7
chelated mesoheme	toluene–10% CH_2Cl_2	8×10^6	0.05	5.3×10^7	1.7×10^3	2.8	5×10^{-4}	5.6×10^3	20a
	toluene	1.1×10^7		8.4×10^7	4.8×10^3	4.9			this work
anthracene–7,7-cyclophane–heme (**1b**)	benzene	6×10^6	0.05	6.5×10^7	1.0×10^3	1.4	9×10^{-4}	1.5×10^3	7
anthracene–6,6-cyclophane–heme (**1a**)	benzene	3×10^4	0.05	1×10^5	8×10^2	7×10^2	0.17[e]	4.1×10^3	7
adamantane–6,6-cyclophane–**5**	toluene	9.2×10^3	0.05	1.5×10^5	690[g] (540)	3.0×10^2	0.59[f]	5.3×10^2	this work
13-cyclophane–heme (**2a**)	benzene	6×10^2	0.07				12		5
15-cyclophane–heme (**2b**)	benzene	9.1×10^4	0.04	1.7×10^6	250	15	0.05	3×10^2	5

[a] Data at 20 or 25 °C; see original references. Solubilities used in this table are as follows: benzene and toluene: see ref 21a; toluene–10% CH_2Cl_2: CO, 1×10^{-5} M $torr^{-1}$, O_2, 1.2×10^{-5} M $torr^{-1}$; water and H_2O/MTAB: CO, 1.36×10^{-6} M $torr^{-1}$, O_2, 1.82×10^{-6} M $torr^{-1}$ (ref 21b). [b] Antonini, E.; Brunori, M. "Hemoglobin and Myoglobin in Their Reactions with Ligands"; Elsevier: New York, 1971; pp 225, 263. [c] Wittenberg, J. B.; Appleby, C. A.; Wittenberg, B. A. *J. Biol. Chem.* **1972**, *247*, 527–531. [d] Traylor, T. G.; Berzinis, A. P. *Proc. Natl. Acad. Sci. U.S.A.* **1980**, *77*, 3171–3175. [e] Determined by both titration and kinetic methods. Other values of $P_{1/2}$ were determined by kinetic methods. [f] Determined by direct titration. [g] See text for methods.

Table XIII. Isocyanide and Carbon Monoxide Binding Constants to Heme Model Compounds in Benzene at 23 °C[a,b]

	adamantane–6,6-cyclophane	anthracene–6,6-cyclophane[d]	anthracene–7,7-cyclophane[d]	chelated protoheme[c]	myoglobin[e]
K_B^{RNC}, M^{-1}					
t-BuNC	3.0×10^4	1.5×10^2	8.0×10^4	1.7×10^8	800
TMIC	2.0×10^5	7.0×10^5	7.0×10^8	7.0×10^9	2.5×10^4
	2.0×10^5[f,g]				
	1.4×10^5				
K_B^{CO}, M^{-1}	1.7×10^5[f]	6.0×10^5	1.1×10^8	4.0×10^8	3.0×10^7
K_{RNC}^{RNC}, M^{-1}					
t-BuNC	1.5×10^4	2	900		
TMIC	5.0×10^3	220	$>10^5$		

[a] Values of K_B^{RNC} determined in this work are at 23 °C. Some of the others are at 20 or 25 °C. [b] See ref 16 for definition of K_B^{RNC} etc. [c] Reference 20a. [d] Reference 20b. [e] Reference 39. [f] Toluene. [g] Data are from Figure 2, using CO displacement. The benzene value was obtained from TMIC displacement by CO.

of base concentration and wavelength of measurement at about 0.4 M base, indicating a complete base-on mechanism of association above this concentration. Therefore both structural and kinetic data indicate that the adamantane–heme–cyclophane **5** differs from the 7,7-cyclophane–heme principally in the introduction of a steric effect. We can therefore compare with confidence the steric effects on CO and O_2 binding among these three cyclophanes.

Kinetic Consequences of Distal-Side Steric Effects. In all the cyclophanes that have shown decreased CO affinity, the CO dissociation rate remains essentially constant.[5,6b,7] In our series of cyclophanes the O_2 and RNC dissociation rates also remain virtually constant over a large variation in binding constants. The variation in affinities of RNC molecules of different sizes to heme proteins is also seen to occur without significant change in dissociation rates.[39] These results seem to document our previous conclusions that distal-side steric effects on all ligands are seen exclusively in the association rates. It would therefore seem reasonable to take as a measure of steric effects the change in association rate[1,14] *at constant dissociation rate*. This qualification is necessary because other effects, discussed above, affect both association and dissociation rates. This makes comparisons of heme proteins rather difficult since dissociation rates vary.

Limits of Steric Effects on Diatomic Molecules. In the aromatic cyclophanes steric effects on CO binding are not observed for $n \geq 7$ in *n,n,...*cyclophanes. Thus neither the 7,7-cyclophane **1b** nor the 7,7,7,7- or 8,8,8,8-capped hemes **4a,b** studied by Rose et al.[9] display any steric hindrance to CO binding, whereas the anthracene–heme–6,6-cyclophane **1a** and adamantane–heme–cyclophane (**5**) show rather larger steric effects toward both CO and O_2. The (5,5,5) "pocket heme" reported by Collman et al.[6] should, by these criteria, have a rather large steric effect on both CO and O_2 binding. While, relative to the parent Fe(TpivPP) complexes there is no effect on O_2 affinity, there is on CO affinity. However, there is a larger effect on dioxygen binding kinetics than on CO kinetics.[6b]

In the alkyl–cyclophane series studied by Ward et al.[5] the 13-, 14-, and 15-cyclophanes (strapped hemes) all show steric effects toward CO binding but the effect in the 15-cyclophane is rather small. We expect that this effect would disappear in the 16-cyclophane, which would be approximately equivalent to a 7,7-cyclophane. Thus the limits on steric hindrance to diatomic molecules seems to be *n,n...* < 7,7,..., or $n < 16$, as suggested by Hashimoto and Basolo.[9b]

Pocket Shape and the Binding of Isocyanides. We previously noted that the anthracene–heme–6,6-cyclophane showed about the same affinity for *n*-butyl- and *tert*-butyl isocyanides as does myoglobin but an affinity for tosylmethyl isocyanide that is greater than that of myoglobin.[37] We attributed this to a peripheral steric effect in the myoglobin pocket that involved groups somewhat further from the heme than the first three atoms. Table XIII, which compares isocyanide binding to different hindered models, further illustrates the importance of the pocket shape. Thus, *tert*-butyl isocyanide suffers a 10^6-fold decrease in affinity in going from chelated heme to anthracene–heme–6,6-cyclophane (**1a**) but only a (6×10^3)-fold decrease in going to the adamantane–heme–6,6-cyclophane (**5**). By contrast, the adamantane–heme–cyclophane shows a slightly greater steric hindrance toward the binding of tosylmethyl isocyanide or carbon monoxide than does the anthracene–6,6-cyclophane. Examination of the structure of **5P** affords a rationale for these results. The CH_2 group closest to the center of the porphyrin is to one side of the ligand and extends upward only about 3.5 Å, thus severely interfering with

(39) Blanck, J.; Ruckpaul, K.; Scheler, W.; Jung, F. *Eur. J. Biochem.* **1972**, *25*, 476–482.

only the first and second atoms (a peripheral steric effect). However, the *tert*-butyl group does encounter some interaction with the adamantane group, as there is NMR evidence for restricted rotation of this group. By comparison, the (2×10^2)-fold greater reduction in *tert*-butyl isocyanide binding to the anthracene–heme–6,6-cyclophane compared with the adamantane–heme–6,6-cyclophane perhaps is a result of the anthracene "roof" being unable to swing to one side of the ligation area. In this instance there would be steric hindrance directly above the iron atom (a central steric effect). The anthracene–heme–7,7-cyclophane is almost as effective in preventing *tert*-butyl isocyanide binding as is the adamantane–heme–6,6-cyclophane, even though the two complexes differ by about 8×10^2 with regard to CO binding. The most striking effect of steric differentiation is seen in the $K_B^{CO}/K_B^{t\text{-BuNC}}$ comparison. This ratio goes from 1.4×10^3 to 4×10^3 to 6 in the series anthracene–7,7-cyclophane, anthracene–6,6-cyclophane, adamantane–6,6-cyclophane. It is 2 for chelated protoheme. Hence the adamantane–cyclophane does not effectively differentiate *t*-BuNC from CO by a steric effect.

The size of the steric effect for a given ligand depends upon the particular cyclophane cap, the adamantane- and alkyl-cyclophanes providing side hindrance (peripheral effect) and the anthracene–cyclophanes providing a roof (central effect). Thus, as for the heme proteins, by proper design of the model system, for example the cyclophane–heme, large ligands can be specifically differentiated by steric effects on the basis of both their size and shape. This corroborates the general idea of steric differentiation of ligands by size and shape.[1,6,12,13,40]

Steric Effects on Dioxygen Binding. In the series anthracene–heme–7,7-cyclophane (**1b**), anthracene–heme–6,6-cyclophane (**1a**), and adamantane–heme–6,6-cyclophane (**5**), the dioxygen dissociation rate changes little, although all these hemes, like the strapped hemes (**2a,b**), have lower values of $k_B^{-O_2}$ than do simple hemes, such as chelated mesoheme. Therefore, the hindered hemes **1a** and **5** can be compared with the unhindered heme **1b** directly. In this series the $P_{O_2}^{1/2}$ values increase from 1.4 torr to 7×10^2 and 3.0×10^2 torr, respectively, while the *M* value, $K_B^{CO}/K_B^{O_2}$, changes from 1.5×10^3 to 4.1×10^3 to 5.3×10^2. By the criterion of the *M* value[18] there seems to be little, if any, steric discrimination between CO and O_2. With the association rates as measures of the distal steric effects,[1] there appears to be a small discrimination against CO in the adamantane–heme **5**. The ratios $k_B^{O_2}/k_B^{CO}$ are 10, 3, and 16 for **1b**, **1a**, and **5**, respectively. The effect is, however, very small. Therefore, neither the anthracene cap, which displays a central steric effect toward isocyanide, nor the adamantane cap, which displays a peripheral steric effect toward isocyanide, shows significant steric differentiation between CO and O_2 binding.

Conformational Effects. The crystal structure of the adamantane–porphyrin–cyclophane **5P** clearly indicates that the adamantane group must move to accommodate ligands. A similar situation exists in deoxyhemoglobin.[4] The adamantane group is in rapid conformational equilibrium in the deoxy form and only a fraction of the conformations are sufficiently open for ligand binding. Once the ligand is bound, some of the conformations are no longer available.

The geometry of the bound CO in **5** is not known. However, its dissociation rate is not accelerated relative to unstrained systems. We conclude that even at these high levels of distal-side steric hindrance the bound state is not particularly strained and the binding constant is controlled by association rates.

Acknowledgment. We are grateful to the National Institutes of Health, Grants HL-13581 (T.G.T.) and HL-13157 (J.A.I.), for support of this research and Grant RR-00757 for support of the computer facilities that were used in this study.

Registry No. 1a, 78505-28-9; **1b**, 78505-29-0; **2a**, 90552-84-4; **2b**, 90531-33-2; **5**, 90531-22-9; **5P**, 90531-20-7; **5P**·$2Cl_2CH_2$, 90531-21-8; **5**-DCIm, 90531-23-0; **5**-DCImCO, 90531-24-1; **5**-MeImCO, 90531-25-2; **5**-Me_2Im, 90531-26-3; **5**-Me_2ImCO, 90531-27-4; **5**-*t*-BuNC, 90531-28-5; **5**-(*t*-BuNC)$_2$, 90531-29-6; **5**-(*t*-BNC)(MeIm), 90531-30-9; **5**-*n*-BuNC, 90531-31-0; **5**-(*n*-BuNC)$_2$, 90531-32-1; O_2, 7782-44-7; CO, 630-08-0; TMIC, 36635-61-7; 8,18-bis(2-carbobenzoxyethyl)-3,13-bis(3-aminopropyl)-2,7,12,17-tetramethylporphyrin, 90552-83-3; chelated mesoheme, 53814-06-5; *tert*-butyl isocyanide, 7188-38-7; 1,3-adamantanediacetyl chloride, 31898-14-3.

Supplementary Material Available: Table III, thermal parameters for the non-hydrogen atoms of 1,3-adamantane–3,13-porphyrin–6,6-cyclophane; Table IV, positional and thermal parameters for the hydrogen atoms of 1,3-adamantane–3,13-porphyrin–6,6-cyclophane; Table V, structure amplitudes; Table VIII, least-squares planes for 1,3-adamantane–3,13-porphyrin–6,6-cyclophane; Table IX, torsion angles for 1,3-adamantane–3,13-porphyrin–6,6-cyclophane (34 pages). Ordering information is given on any current masthead page.

(40) St. George, R. C. C.; Pauling, L. *Science (Washington, D.C.)* **1951**, *114*, 629–634.

Generation of Binuclear $(d^8 \cdot d^8)p\sigma$ Platinum and Rhodium Complexes by Pulse Radiolysis

Chi-Ming Che,[1a] Stephen J. Atherton,[1b] Leslie G. Butler,[1c] and Harry B. Gray*

Contribution No. 6956 from the Arthur Amos Noyes Laboratory, California Institute of Technology, Pasadena, California 91125. *Received December 7, 1983*

Abstract: Two $(d^8 \cdot d^8)p\sigma$ binuclear complexes, $Pt_2(pop)_4^{5-}$ (pop = $P_2O_5H_2^{2-}$) and $Rh_2(TMB)_4^{+}$ (TMB = 2,5-dimethyl-2,5-diisocyanohexane), have been generated by pulse radiolysis of aqueous and acetonitrile solutions, respectively, of the corresponding $d^8 \cdot d^8$ species. An intense absorption system attributable to the allowed $d\sigma^* \rightarrow p\sigma$ transition is observed in the spectrum of each of the transients (420 nm, $Pt_2(pop)_4^{5-}$; 570 nm, $Rh_2(TMB)_4^{+}$).

In 1980 we reported that Rh_2^{+} species could be produced by reductive quenching of the $^3d\sigma^*p\sigma$ states of $Rh_2(TMB)_4^{2+}$ and $Rh_2b_4^{2+}$ (TMB = 2,5-dimethyl-2,5-diisocyanohexane; b = 1,3-diisocyanopropane).[2] At the time the transient absorption spectra of these species could not be established unambiguously, because of the absorptions of the oxidized quenchers. We have now found that $Rh_2(TMB)_4^{+}$ and a binuclear platinum analogue, $Pt_2(pop)_4^{5-}$ (pop = $P_2O_5H_2^{2-}$), can be generated by pulse radiolysis of solutions containing their $d^8 \cdot d^8$ parents. The absorption spectra of these

(1) Present address: (a) Department of Chemistry, University of Hong Kong, Pokfulam Road, Hong Kong. (b) Center for Fast Kinetics Research, The University of Texas, Austin, Texas 78712. (c) Department of Chemistry, Louisiana State University, Baton Rouge, Louisiana 70803.

(2) Milder, S. J.; Goldbeck, R. A.; Kliger, D. S.; Gray, H. B. *J. Am. Chem. Soc.* **1980**, *102*, 6761.

0002-7863/84/1506-5143$01.50/0